Pharmacokinetic Influence of the Dosing Time of Tacrolimus

Tacrolimus (2 mg/kg i.p.) was injected once a day at 8:00 (light group) or 20:00 (dark group). Blood samples were obtained from the abdominal aorta at 0.5, 1, 2, 4, 8, 12, and 24 h after a single injection or 24 h after the 7th injection. Tacrolimus concentrations in whole blood were measured with an enzyme immunoassay (IMx; Abbot Laboratories, Abbot Park, III).

Statistical Analysis

Data are expressed as means ± S.E.M. A one-way analysis of variance (ANOVA) followed by the post hoc Sheffe's F-test was used to analyze the concentrations of BUN, creatinine, and tacrolimus. The duration of harmine-induced tremors and that of skin graft survival were evaluated using the Mann–Whitney U-test and log-rank test, respectively. Statistical significance was defined as $P < 0.05$.

RESULTS

Influence of the Dosing Time of Tacrolimus on Harmine-Induced Tremors and the Serum BUN and Creatinine Concentrations

On the basis of the results of preliminary experiments, the dose of harmine was selected to induce a minimal tremor response (the duration of tremors ranged from 0 to 100 s in the light and dark group). Tacrolimus (2 mg/kg i.p., once a day for 7 days) significantly prolonged harmine-induced tremors 2.7-fold compared to the vehicle in the light group ($P < 0.05$), but not in the dark group (Fig. 1). The facilitatory action of tacrolimus on harmine-induced tremors was greater in the light group than dark group (Fig. 1; $P < 0.05$).

In the light group, tacrolimus (2 mg/kg i.p., once a day for 14 days) increased significantly BUN concentrations by 74.7% (Fig. 2(A), $P < 0.01$) and moderately raised creatinine concentrations by 39.5% (Fig. 2(C)). Tacrolimus-affected BUN levels were significantly higher in the light group than dark group ($P < 0.05$). In the dark group, there were only slight differences in the serum BUN and creatinine concentrations between tacrolimus and vehicle treatment (Fig. 2(B) and 2(D)).

Influence of the Dosing Time of Tacrolimus on Xenograft Survival

Figure 3 shows survival curves of the skin xenograft for the light (A) and dark (B) group. The mouse-to-rat skin graft transplanted in the light phase (vehicle; 14.8 ± 0.6 days) survived for a longer period than that transplanted in the dark phase (vehicle; 12.3 ± 0.5 days). In the dark group, tacrolimus (2 mg/kg i.p.) significantly increased the mean survival time by 20% ($P < 0.05$), leading to almost the same levels as those in the light group treated with vehicle or tacrolimus. In the light group, no significant differences were observed between vehicle and tacrolimus treatment.

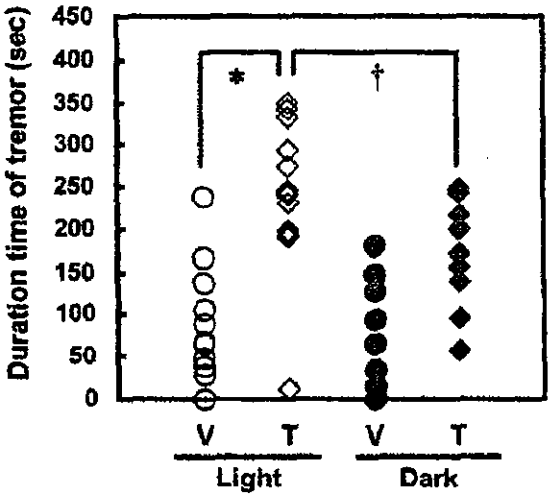

Fig. 1. Influence of the dosing time (8:00 (light) or 20:00 (dark)) of tacrolimus on harmine-induced tremors in rats. The animals were subjected to subchronic treatment with tacrolimus (T) (2 mg/kg i.p.) or vehicle (V) once a day for 7 days. Rats were injected with harmine (10 mg/kg i.p.) 55 min after the final injection of vehicle or tacrolimus. The summed duration of tremors was measured during a 15 min period from 5 to 20 min after harmine injection ($n = 10$–12 per group). $^{*}P < 0.05$; significantly different from the vehicle-treated group. $^{\dagger}P < 0.05$; significantly different from the tacrolimus-treated group in the dark phase.

Pharmacokinetics Influence of the Dosing Time of Tacrolimus After Single or Repeated Injection

The curves for mean tacrolimus concentration versus time after single injections are shown in Fig. 4(A). Tacrolimus levels in whole blood at 1, 4, and 8 h after injection were slightly, although not significantly, higher in the light group than dark group. As shown in Fig. 4(B), the dosing time (light or dark phase) for the repeated injection of tacrolimus had no significant influence on trough levels.

DISCUSSION

The present study demonstrated that the repeated injection of tacrolimus in the light phase (8:00) produced a significantly greater increase than that in the dark phase (20:00) in the duration of harmine-induced tremors and in BUN concentrations in rats. An immunosuppressive effect of tacrolimus on the xenotransplantation of a mouse-to-rat skin graft was apparent in the dark phase but not in the light phase. These findings suggest that treatment in the dark phase (an active phase in the rat diurnal rhythm) ameliorates the neurotoxicity and nephrotoxicity while maintaining the immunosuppressive effect of tacrolimus in rats.

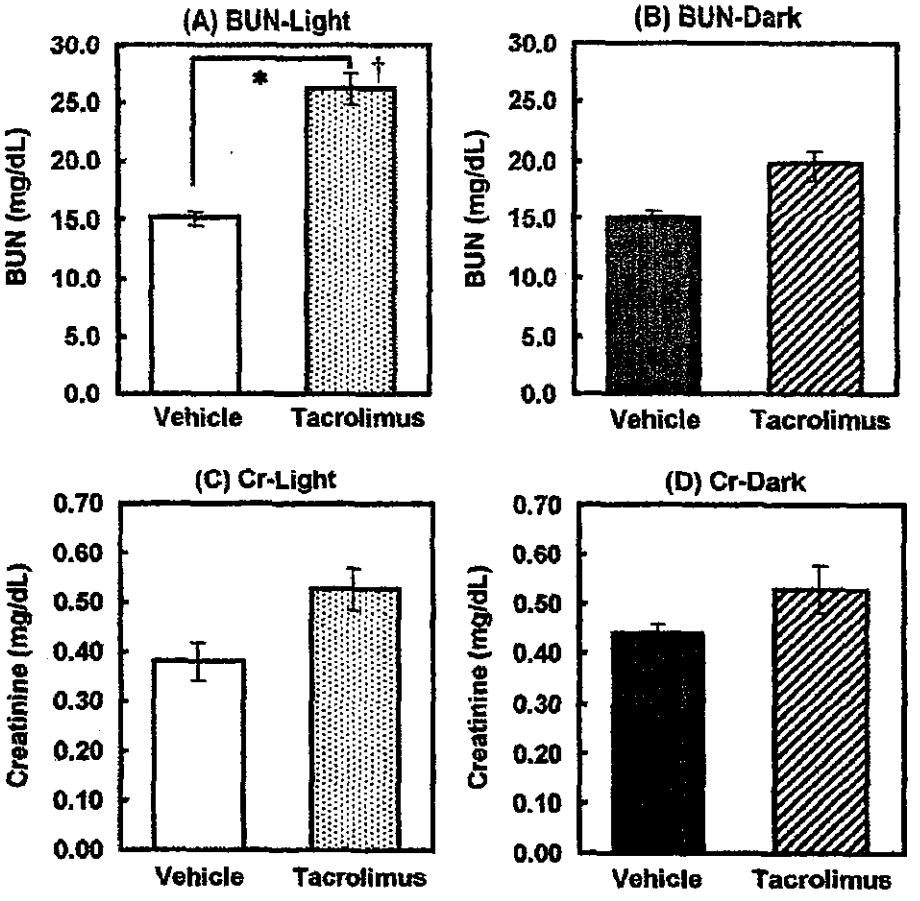

Fig. 2. Influence of the dosing time (8:00 or 20:00) of tacrolimus on the BUN and creatinine concentrations in rats. The animals were subjected to subchronic treatment with tacrolimus (2 mg/kg i.p.) or vehicle once a day for 14 days. Blood samples were collected from the tail vein 24 h after the final tacrolimus injection. Values represent the means ± S.E.M. for 5–7 rats. (A) The BUN concentrations in the light group (BUN-light); (B) The BUN concentrations in the dark group (BUN-dark); (C) The creatinine concentrations in the light group (Cr-light); (D) The creatinine concentrations in the dark group (Cr-dark). $^{**}P < 0.01$; significantly different from the vehicle-treated group. $^{\dagger}P < 0.05$; significantly different from the tacrolimus-treated group in the dark phase.

No chronopharmacological research has been published concerning immunosuppressant-induced neurotoxicity. The present study is the first to provide evidence that a facilitatory action of tacrolimus on harmine-induced tremors shows a diurnal rhythm with a potent effect in the light phase in rats. Harmine is reported to induce tremors by activating serotonergic neurons and inhibiting dopaminergic neurons (Kawanishi *et al.*, 1981). Shuto *et al.* (1998) demonstrated that cyclosporine facilitates serotonergic neural activity to accelerate harmine-induced tremors. This acceleration appeared to be involved in an inhibition of γ-aminobutyric acid neural activity and receptors (Shuto *et al.*, 1999; Tominaga *et al.*, 2001). The precise mechanisms by which tacrolimus neurotoxicity exhibits a diurnal rhythm remains to be determined.

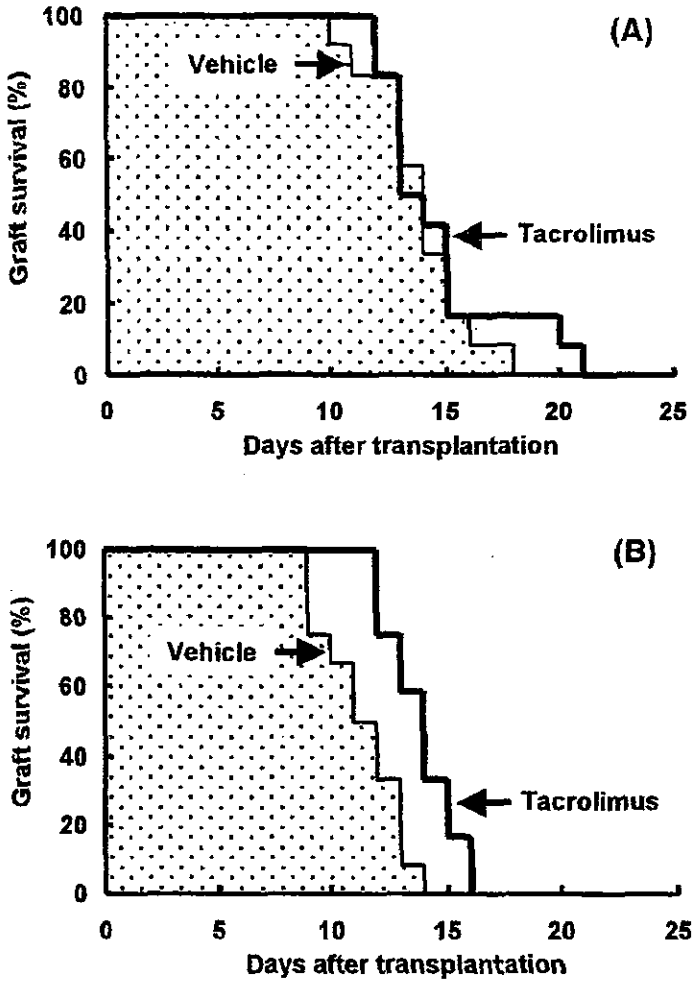

Fig. 3. Influence of the dosing time (8:00 (A) and 20:00 (B)) of tacrolimus on the survival of skin xenografts in a mouse-to-rat skin xenotransplantation model. The animals were subjected to chronic treatment with tacrolimus (2 mg/kg i.p., thick line) or vehicle (thin line and dotted area) once a day until rejection of the graft occurred. Rejection was defined as a complete separation of the graft in each rat. Data are expressed as the percentage of rats in which the graft survived in each group (12 rats each). $^*P < 0.05$; significantly different from the vehicle-treated group.

The dosing time-dependent nephrotoxicity of tacrolimus in rats was previously reported by Fujimura and Ebihara (1994). Contrary to our findings, they showed that the tacrolimus-induced elevation in the BUN and creatinine levels was more prominent in the dark phase than in the light phase in rats. Their pharmacokinetic results suggested that an aggravation of renal function induced by tacrolimus in the dark phase is closely associated with the high concentrations of tacrolimus in whole blood in the dark phase. This diurnal rhythm was not observed in the present pharmacokinetic study. The discrepancy in these findings may be due to the different route of administration (an intraperitoneal route in our study versus an oral route

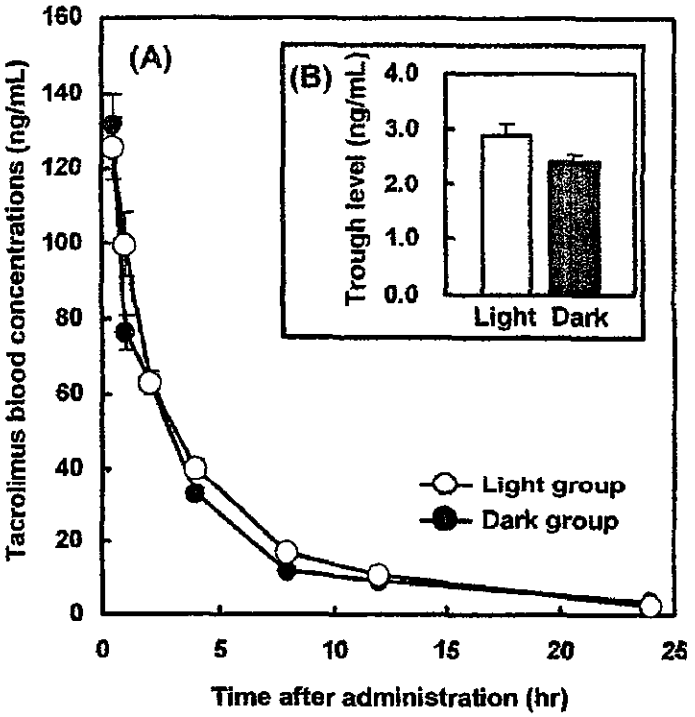

Fig. 4. The pharmacokinetic influence of the dosing time (8:00 (light) or 20:00 (dark)) of tacrolimus (2 mg/kg i.p.) after a single (A) or repeated (B) injection. Blood samples were obtained from the abdominal aorta at 0.5, 1, 2, 4, 8, 12, and 24 h after a single injection or 24 h after repeated injection (once a day for 7 days). Values represent means ± S.E.M. for 5–6 rats.

in Fujimura's study). In the oral administration of tacrolimus, the maximum concentration or area under the concentration–time curve (AUC) of tacrolimus was significantly increased when tacrolimus was given in the morning in humans or in the dark phase in nocturnal rodents (Fujimura *et al.*, 1993, Min *et al.*, 1996, Uchida *et al.*, 1999). These phenomena seem to be caused by several diurnal rhythm-related variables including food ingestion, gastric emptying time, gastric motility, secretion of bile acid, blood flow to the gastrointestinal tract, and gastrointestinal perfusion. In the present study, the dosing time-dependent influences are not involved in tacrolimus absorption, since tacrolimus was intraperitoneally administered. Interestingly, the AUC of tacrolimus on continuous intravenous administration in humans showed no differences between daytime and nighttime (Satoh *et al.*, 2001). This is consistent with our results suggesting that the pharmacokinetic features of tacrolimus following parenteral administration probably indicate no circadian variation. Therefore, the pharmacokinetic factors may be excluded from the mechanisms of diurnal changes in tacrolimus-induced toxicity and efficacy in the present study. The possibility that the distribution of tacrolimus in the kidney and brain has diurnal variations remains to be examined.

Calcineurin inhibitors including tacrolimus and cyclosporine exert an immunosuppressive action due to the inhibition of interleukin (IL)-2 transcription, leading

to T cell inactivation (Liu, 1993; Wiederrecht *et al.*, 2000). Since a diurnal rhythm exists in the secretion of IL-2 or the number of T cells (Born *et al.*, 1997; Palm *et al.*, 1996), the immunosuppressive effects of calcineurin inhibitors are speculated to depend on the dosing time during the day. In the present study, the administration of tacrolimus in the dark phase significantly prolonged the survival time of skin grafts in the xenograft transplantation model. These findings were supported by a report concerning the effect of cyclosporine on a murine heart allograft model (Cavallini *et al.*, 1983). The efficacy of tacrolimus or cyclosporine is likely to increase when the agent is administered in the dark phase in the rodents.

In conclusion, we provided evidence that treatment in the active phase ameliorates the neurotoxicity and nephrotoxicity while maintaining the immunosuppressive effect of tacrolimus in rats. The present findings have important implications for therapeutic approaches to avoid tacrolimus-induced neurotoxicity and nephrotoxicity.

ACKNOWLEDGMENTS

We thank Y. Isotani and K. Toda for assistance. This work was supported in part by a Grant-in-aid for Scientific Research ((B)(2) 14370789) from the Ministry of Education, Culture, Sports, Science, and Technology (MEXT), Japan and by funds (No.: 031001) from the Central Research Institute of Fukuoka University.

REFERENCES

Bobadilla, N. A., Gamba, G., Tapia, E., Garcia-Torres, R., Bolio, A., López-Zetina, P., and Herrera-Acosta, J. (1998). Role of NO in cyclosporin nephrotoxicity: Effects of chronic NO inhibition and NO synthases gene expression. *Am. J. Physiol.* **274**:F791–F798.

Born, J., Lange, T., Hansen, K., Mölle, M., and Fehm, H. L. (1997). Effects of sleep and circadian rhythm on human circulating immune cells. *J. Immunol.* **158**:4454–4464.

Brandenberger, G., Follenius, M., Goichot, B., Saini, J., Spiegel, K., Ehrhart, J., and Simon, C. (1994). Twenty-four-hour profiles of plasma renin activity in relation to the sleep-wake cycle. *J. Hypartens.* **12**:277–283.

Cardinali, D. P., and Golombek, D. A. (1998). The rhythmic GABAergic system. *Neurochem. Res.* **23**:607–614.

Cavallini, M., Magnus, G., Halberg, F., Tao, L., Field, M. Y., Sibley, R., Najarian, J. S., and Sutherland, D. E. R. (1983). Benefit from circadian timing of cyclosporine revealed by delay of rejection of murine heart allograft. *Transplant. Proc.* **15**(Suppl. 1):2960–2966.

European FK506 Multicentre Liver Study Group. (1994). Randomised trial comparing tacrolimus (FK506) and cyclosporin in prevention of liver allograft rejection. *Lancet.* **344**:423–428.

Fujimura, A., and Ebihara, A. (1994). Administration time-dependent toxicity of a new immunosuppressive agent, tacrolimus (FK506). *Life Sci.* **55**:485–490.

Fujimura, A., Shiga, T., Ohashi, K., and Ebihara, A. (1993). Chronopharmacokinetic study of a new immunosuppressive agent, FK506, in mice. *Jpn. J. Pharmacol.* **61**:137–139.

Fujisaki, Y., Yamauchi, A., Dohgu, S., Sunada, K., Yamaguchi, C., Oishi, R., and Kataoka, Y. (2002). Cyclosporine A-increased nitric oxide production in the rat dorsal hippocampus mediates convulsions. *Life Sci.* **72**:549–556.

Hutson, P. H., Sarna, G. S., and Curzon, G. (1984). Determination of daily variations of brain 5-hydroxytryptamine and dopamine turnovers and of the clearance of their acidic metabolites in conscious rats by repeated sampling of cerebrospinal fluid. *J. Neurochem.* **43**:291–293.

Hwang, Y. S., Hsieh, T. J., Lee, Y. J., and Tsai, J. H. (1998). Circadian rhythm of urinary endothelin-1 excretion in mild hypertensive patients. *Am. J. Hypertens.* **11**:1344–1351.

Ikesue, H., Kataoka, Y., Kawachi, R., Dohgu, S., Shuto, H., and Oishi, R. (2000). Cyclosporine enhances α1-adrenoceptor-mediated nitric oxide production in C6 glioma cells. *Eur. J. Pharmacol.* **407:**221–226.

Isram, M., Burke, J. F., Jr., McGowan, T. A., Zhu, Y., Dunn, S. R., McCue, P., Kanalas, J., and Sharma, K. (2001). Effect of anti-transforming growth factor-beta antibodies in cyclosporine-induced renal dysfunction. *Kidney Int.* **59:**498–506.

Kawanishi, K., Hashimoto, Y., Fujiwara, M., Kataoka, Y., and Ueki, S. (1981). Pharmacological characteristics of abnormal behavior induced by harmine with special reference to tremor in mice. *J. Pharm. Dyn.* **4:**520–527.

Kupferman, J. C., Beaudoin, R., Carr, R., Hay, D., Casellas, D., Kaskel, F. J., and Moore, L. C. (1994). Activation of the renal renin-angiotensin system by cyclosporine A and FK 506 in the rat. *Transplant. Proc.* **26:**2891–2893.

Lanese, D. M., and Conger J. D. (1993). Effects of endothelin receptor antagonist on cyclosporine-induced vasoconstriction in isolated rat renal arterioles. *J. Clin. Invest.* **91:**2144–2149.

Lanese, D. M., Falk, S. A., and Conger J. D. (1994). Sequential agonist activation and site-specific mediation of acute cyclosporine constriction in rat renal arterioles. *Transplantation* **58:**1371–1378.

Levi, F., Zidani, R., and Misset, J. L. (1997). Randomised multicentre trial of chronotherapy with oxaliplatin, fluorouracil, and folinic acid in metastatic colorectal cancer. *Lancet* **350:**681–686.

Liu, J. (1993). FK506 and cyclosporin, molecular probes for studying intracellular signal transduction. *Immunol. Today* **14:**290–295.

Min, D. I., Chen, H. Y., Fabrega, A., Ukah, F. O., Wu, Y. M., Corwin, C., Ashton, M. K., and Martin, M. (1996). Circadian variation of tacrolimus disposition in liver allograft recipients. *Transplantation* **62:**1190–1192.

Ohdo, S., Koyanagi, S., Suyama, H., Higuchi, S., and Aramaki, H. (2001). Changing the dosing schedule minimizes the disruptive effects of interferon on clock function. *Nat. Med.* **7:**356–360.

Palm, S., Postler, E., Hinrichsen, H., Maier, H., Zabel, P., and Kirch, W. (1996). Twenty-four-hour analysis of lymphocyte subpopulations and cytokines in healthy subjects. *Chronobiol. Int.* **13:**423–434.

Satoh, S., Tada, H., Tachiki, Y., Tsuchiya, N., Shimoda, N., Akao, T., Sato, K., Habuchi, T., Suzuki, T., and Kato, T. (2001). Chrono and clinical pharmacokietic study of tacrolimus in continuous intravenous administration. *Int. J. Urol.* **8:**353–358

Shapira, O. M., Rene, H., Lider, O., Pfeffermann, R. A., Shemin, R. J., and Cohen, I. R. (1999). Prolongation of rat skin and cardiac allograft survival by low molecular weight heparin. *J. Surg. Res.* **85:**83–87.

Shuto, H., Kataoka, Y., Fujisaki, K., Nakao, T., Sueyasu, M., Miura, I., Watanabe, Y., Fujiwara, M., and Oishi, R. (1999). Inhibition of GABA system involved in cyclosporine-induced convulsions. *Life Sci.* **65:**879–887.

Shuto, H., Kataoka, Y., Kanaya, A., Matsunaga, K., Sueyasu, M., and Oishi, R. (1998). Enhancement of serotonergic neural activity contributes to cyclosporine-induced tremors in mice. *Eur. J. Pharmacol.* **341:**33–37.

Snyder, S. H., Sabatini, D. M., Lai, M. M., Steinet, J. P., Hamilton, G. S., and Suzdak, P. D. (1998). Neuronal actions of immunophilin ligands. *Trends Pharmacol. Sci.* **19:**21–26.

Steiner, J. P., Dawson, T. M., Fotuhi, M., and Snyder, S. H. (1996). Immunophilin regulation of neurotransmitter release. *Mol. Med.* **2:**325–333.

The U.S. Multicenter FK506 Liver Study Group. (1994). A comparison of tacrolimus (FK 506) and cyclosporine for immunosuppression in liver transplantation. *N. Engl. J. Med.* **331:**1110–1115.

Tominaga, K., Yamauchi, A., Shuto, H., Niizeki, M., Makino, K., Oishi, R., and Kataoka, Y. (2001). Ovariectomy aggravates convulsions and hippocampal γ-aminobutyric acid inhibition induced by cyclosporin A in rats. *Eur. J. Pharmacol.* **430:**243–249.

Uchida, H., Kobayashi, E., Ogino, Y., Mizuta, K., To, H., Okabe, R., Hashizume, K., and Fujimura, A. (1999). Chronopharmacology of tacrolimus in rats: Toxicity and efficacy in a mouse-to-rat intestinal transplant model and its pharmacokinetic profile. *Transplant. Proc.* **31:**2751–2753.

Wiederrecht, G., Lam, E., Hung, S., Martin, M., and Sigal, N. (2000). The mechanism of action of FK-506 and cyclosporin A. *Ann. N. Y. Acad. Sci.* **696:**9–19.

Cellular and Molecular Neurobiology, Vol. 24, No. 3, June 2004 (© 2004)

Rapid Communication

Transforming Growth Factor-β1 Upregulates the Tight Junction and P-glycoprotein of Brain Microvascular Endothelial Cells

Shinya Dohgu,[1,2] Atsushi Yamauchi,[2] Fuyuko Takata,[2] Mikihiko Naito,[3] Takashi Tsuruo,[3] Shun Higuchi,[1] Yasufumi Sawada,[1] and Yasufumi Kataoka[2,4]

Received September 29, 2003; accepted October 10, 2003

SUMMARY

1. The present study was aimed at elucidating effects of transforming growth factor-β (TGF-β) on blood–brain barrier (BBB) functions with mouse brain capillary endothelial (MBEC4) cells.

2. The permeability coefficients of sodium fluorescein and Evans blue albumin for MBEC4 cells and the cellular accumulation of rhodamine 123 in MBEC4 cells were dose-dependently decreased after a 12-h exposure to TGF-β1 (0.01–10 ng/mL).

3. The present study demonstrates that TGF-β lowers the endothelial permeability and enhances the functional activity of P-gp, suggesting that cellular constituents producing TGF-β in the brain may keep the BBB functioning.

KEY WORDS: transforming growth factor-β; blood–brain barrier; permeability; P-glycoprotein; mouse brain endothelial cells.

INTRODUCTION

The Blood–brain barrier (BBB) is highly restrictive of the transport of substances between blood and the central nervous system. The BBB is a complex system of different cellular component consisting brain microvascular endothelial cells, pericytes

[1] Department of Medico-Pharmaceutical Sciences, Graduate School of Pharmaceutical Sciences, Kyushu University, Higashi-ku, Fukuoka, Japan.
[2] Department of Pharmaceutical Care and Health Sciences, Faculty of Pharmaceutical Sciences, Fukuoka University, Jonan-ku, Fukuoka, Japan.
[3] Institute of Molecular and Cellular Biosciences, University of Tokyo, Bunkyo-ku, Tokyo, Japan.
[4] To whom correspondence should be addressed at Department of Pharmaceutical Care and Health Sciences, Faculty of Pharmaceutical Sciences, Fukuoka University, 8-19-1 Nanakuma, Jonan-ku, Fukuoka 814-0180, Japan; e-mail: ykataoka@cis.fukuoka-u.ac.jp.

0272-4340/04/0600-0491/0

and astrocytes. Astrocytes induce and maintain the properties of the BBB including the integration of tight junctions and expression of P-glycoprotein (P-gp) through cell-to-cell contact and secretion of soluble factors (Rubin and Staddon, 1999). Brain pericytes are important for the control of growth and migration of endothelial cells and the integrity of microvascular capillaries (Ramsauer *et al.*, 2002). These functions are mediated, at least in part, by transforming growth factor-β (TGF-β), a family of multifunctional peptide growth factors (Orlidge and D'Amore, 1987; Sato and Rifkin, 1989). TGF-β isoforms (TGF-β1, 2, 3, 4, and 5) share the same structure (65–80% homology) and display similar biological activity in vitro (Flanders *et al.*, 1998). TGF-β is listed as a compound protecting against neurodegeneration (Flanders *et al.*, 1998). Several cytokines and growth factors influence on the permeability of the BBB, such as vascular endothelial growth factor (Wang *et al.*, 1996) and tumor necrosis factor-α (Deli *et al.*, 1995). However, little is known about the role of TGF-β in the maintenance of BBB function. In the present study, effects of TGF-β1 were examined on the permeability of brain endothelial cells and the functional activity of P-gp. We used mouse brain endothelial (MBEC4) cells showing the highly specialized characteristics of brain microvascular endothelial cells including the expression of P-gp (Tatsuta *et al.*, 1992, 1994).

MATERIALS AND METHODS

MBEC4 cells, which were isolated from BALB/c mouse brain cortices and immortalized by SV40-transformation (Tatsuta *et al.*, 1992), were cultured in Dulbecco's modified Eagle's medium (DMEM) (GIBCO BRL, Life Technologies, Grand Island, NY) supplemented with 10% fetal bovine serum, 100 units/mL of penicillin, and 100 μg/mL of streptomycin. They were grown in 12-well Transwells^{TM} (Costar, MA) and 24-well plates (FALCON; Becton Dickinson Labware, Lincolin Park, NJ) in a humidified atmosphere of 5% CO_2/95% air at 37°C.

MBEC4 cells (42,000 cells/cm^2) were cultured on the collagen-coated polycarbonate membrane (3.0 μm pore size) of the Transwell^{TM} insert (12-well type). After culture for 3 days, they were washed three times with serum-free medium. Cells were exposed to 0.01–10 ng/mL of TGF-β1 (Sigma, St. Louis) injected into the inside of the insert (luminal side) for 12 h. To initiate the transport experiments, the medium was removed and cells were washed three times with Krebs–Ringer buffer (118 mM NaCl, 4.7 mM KCl, 1.3 mM $CaCl_2$, 1.2 mM $MgCl_2$, 1.0 mM NaH_2PO_4, 25 mM $NaHCO_3$, and 11 mM D-glucose, pH 7.4). Krebs–Ringer buffer (1.5 mL) was added outside of the insert (abluminal side). Krebs–Ringer buffer (0.5 mL) containing 100 μg/mL of sodium fluorescein (Na-F) (MW 376, Sigma, St. Louis) and 4% bovine serum albumin (Sigma, St. Louis) mixed with 0.67 mg/mL of Evans blue dye (EBA) (MW 67,000, Wako, Osaka, Japan) was loaded on the luminal side of the insert. Samples (0.5 mL) were removed from the abluminal chamber at 10, 20, 30, and 60 min and immediately replaced with fresh Krebs–Ringer buffer. Aliquots (5 μL) from the abluminal chamber samples were mixed with 200 μL of Krebs–Ringer buffer and then the concentration of Na-F was determined using a multiwell fluorometer (Ex(λ) 485 nm; Em(λ) 530 nm) (CytoFluor Series 4000, PerSeptive Biosystems, Framingham, MA).

The EBA concentration in the abluminal chamber was measured by determining the absorbance of aliquots (150 μL) at 630 nm with a microplate reader (Opsys MR, DYNEX technologies, Chantilly, VA). The permeability coefficient and clearance were calculated according to the method described by Dehouck *et al.* (1992). Clearance was expressed as microliter (μL) of tracer diffusing from the luminal to abluminal chamber and was calculated from the initial concentration of tracer in the luminal and final concentration in the abluminal chamber: Clearance (μL) = $[C]_A \times V_A/[C]_L$ where $[C]_L$ is the initial luminal tracer concentration, $[C]_A$ is the abluminal tracer concentration, and V_A is the volume of the abluminal chamber. During a 60-min period of the experiment, the clearance volume increased linearly with time. The average volume cleared was plotted versus time, and the slope was estimated by linear regression analysis. The slope of clearance curves for the MBEC4 monolayer was denoted PS_{app}, where PS is the permeability $\times$ surface area product (in μL/min). The slope of the clearance curve with a control membrane was denoted $PS_{membrane}$. The real PS value for the MBEC4 monolayer (PS_{trans}) was calculated from $1/PS_{app} = 1/PS_{membrane} + 1/PS_{trans}$. The PS_{trans} values were divided by the surface area of the Transwell inserts to generate the permeability coefficient (P_{trans}, in cm/min).

The functional activity of P-gp was determined by measuring the cellular accumulation of rhodamine 123 (Sigma, St. Louis) according to the method of Fontaine *et al.* (1996). MBEC4 cells (21,000 cells/cm^2) were cultured on the collagen-coated 24-well plates. Three days after seeding cells, they were washed three times with serum-free medium and then exposed to 0.01–10 ng/mL of TGF-β1 for 12 h. The medium was removed and cells were washed three times with assay buffer (143 mM NaCl, 4.7 mM KCl, 1.3 mM $CaCl_2$, 1.2 mM $MgCl_2$, 1.0 mM NaH_2PO_4, 10 mM HEPES, and 11 mM D-glucose, pH 7.4). Cells were incubated with 0.5 mL of assay buffer containing 5 μM rhodamine 123 for 1 h. Then, the solution was removed and cells were washed three times with ice-cold phosphate-buffered saline and solubilized in 0.2 N NaOH (0.5 mL). The rhodamine 123 content was determined using a multiwell fluorometer (Ex(λ) 485 nm; Em(λ) 530 nm) (CytoFluor Series 4000, PerSeptive Biosystems, Framingham, MA). The cellular protein was measured by the method of Bradford (1976).

The values are expressed as means $\pm$ SEM. Statistical analysis was performed using Student's unpaired *t* test. A single-factor analysis of variance (ANOVA) followed by the Dunnett test was applied to multiple comparisons. The differences between means were considered to be significant when *P* values were less than 0.05.

RESULTS

TGF-β1 at a concentration of 10 ng/mL significantly decreased the permeability of the cells to Na-F and EBA at 3 h by 71.9 and 55.5% of control, respectively, during a period of 6–12 h (Fig. 1(A) and (B)). The permeability coefficients of Na-F and EBA for MBEC4 cells were dose-dependently reduced by 1.7–38.8% and 8.4–42.1%, respectively, after a 12-h exposure to TGF-β1 (0.01–10 ng/mL) (Fig. 1(A) and (B)). As shown in Fig. 2, the cellular accumulation of rhodamine 123 into MBEC4 cells was dose-dependently reduced by 69.0–100.7%

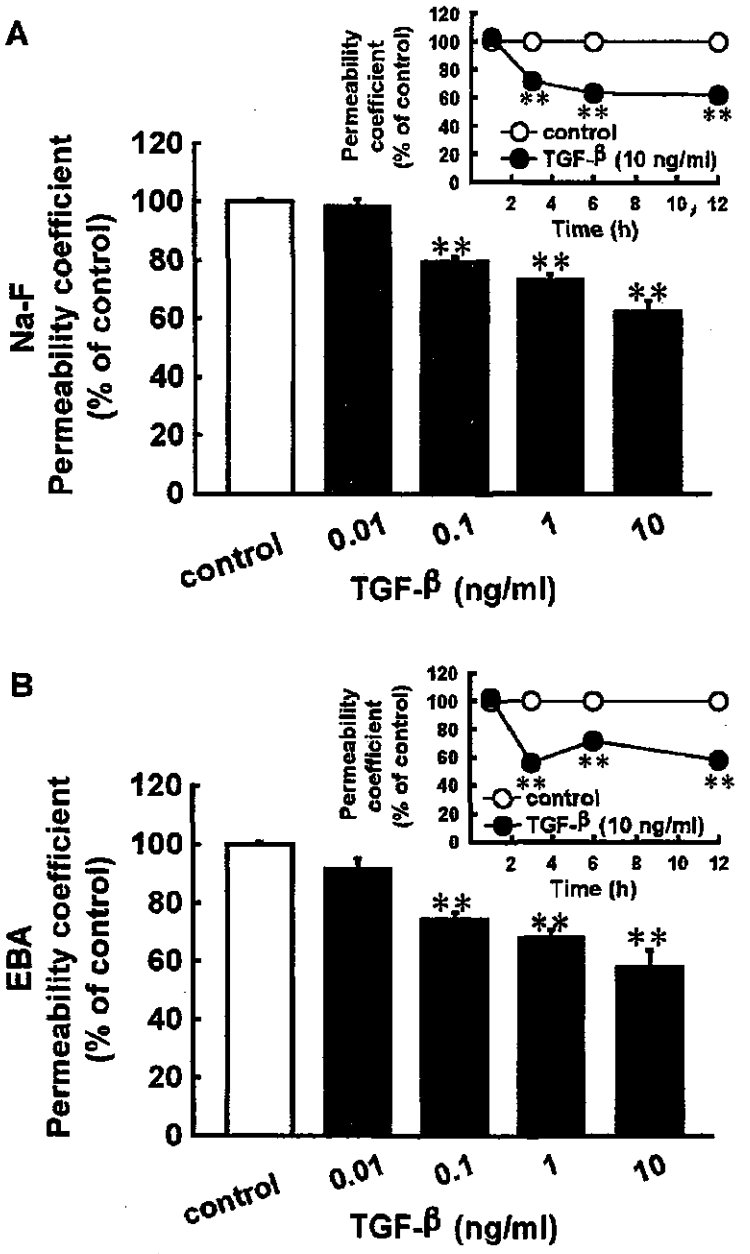

Fig. 1. Changes in the permeability coefficient of Na-F (A) and EBA (B) in MBEC4 cell monolayers after exposure to various concentrations of TGF-β1 for 12 h. The permeability coefficients of Na-F and EBA for the control in panel A and B were 2.71 ± 0.09 × 10^{-4} and 0.85 ± 0.05 × 10^{-4} cm/min, respectively. The inset in each panel shows the time-course of the permeability coefficient of Na-F and EBA after exposure to 10 ng/mL of TGF-β1. The permeability coefficients of Na-F and EBA for the control were 1.34 ± 0.02, 2.10 ± 0.05, 2.17 ± 0.01, and 3.01 ± 0.13 × 10^{-4} cm/min in the inset of panel A (Na-F) for 1, 3, 6, and 12 h, respectively, and 0.46 ± 0.02, 0.97 ± 0.02, 0.66 ± 0.03, and 1.02 ± 0.08 × 10^{-4} cm/min in the inset of panel B (EBA) for 1, 3, 6, and 12 h, respectively. Data are expressed as percentages of control. Values are shown as means ± SEM (n = 4–24). **P < 0.01; significant difference from control.

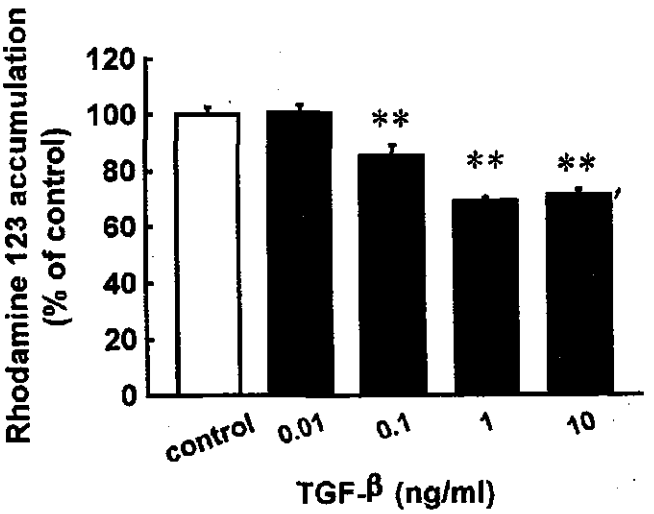

Fig. 2. Changes in the cellular accmulation of rhodamine 123 in MBEC4 cells after exposure to various concentrations of TGF-β1 for 12 h. The cellular accumulation of rhodamine 123 in MBEC4 cells for the control was 1.65 ± 0.05 nmol/mg protein. Data are expressed as percentages of control. Values are shown as means ± SEM (n = 4–10). $^{**}P < 0.01$; significant difference from control.

of control after a 12-h exposure to TGF-β1 at concentrations ranging from 0.1 to 10 ng/mL.

DISCUSSION

The permeability of Na-F and EBA through the MBEC4 monolayer was reduced by TGF-β1 and the accumulation of rhodamine 123 into MBEC4 cells was significantly decreased by TGF-β1. This action of TGF-β1 appeared within 3 h after treatment. These findings suggest that TGF-β1 supports the maintenance of BBB functions by integrating tight junctions and activating a P-gp-related transport system. The epithelial and endothelial barrier of paracellular permeability through tight junctions is known to be regulated by various signaling molecules including protein kinase C. Activation of protein kinase C is involved in the TGF-β signaling pathway (Halstead *et al.*, 1995), leading to a decrease in the permeability of brain microvascular endothelial cells (Raub, 1996). TGF-β-enhanced BBB functions in the early stage may be interpreted as occurring due to protein kinase C activation. TGF-β mediates multifunctional effects by eliciting transcriptional responses in many target genes. TGF-β1 increased *mdr1* gene expression via a protein kinase C-related signal transduction pathway (Utsunomiya *et al.*, 1997). The other TGF-β signaling cascades from membrane to nucleus could be involved in an enhancement of BBB functions, such as mitogen-activated protein kinase (Hartsough and Mulder, 1995) and a receptor serine/threonine kinase pathway (Wrana *et al.*, 1994). It is, therefore,

conceivable that TGF-β facilitates the barrier function and P-gp functional activity of brain endothelial cells by increasing the expression of tight junction-associated proteins (such as occludin and claudins) and P-gp. Endothelial cells, when co-cultured with pericytes, produced an activated form of TGF-β (Antonelli-Olridge *et al.*, 1989) and elevated transendothelial electrical resistance (Dente *et al.*, 2001), suggesting that TGF-β production by pericytes is significant for maintaining the integrity of the BBB.

In the present study, we demonstrated that TGF-β1 lowered endothelial permeability and increased the functional activity of the P-gp efflux pump in MBEC4 cells. These findings suggest that cellular constituents producing TGF-β in the brain may keep the BBB functioning.

ACKNOWLEDGMENTS

This work was supported in part by a Grant-in-Aid for Scientific Research ((B)(2) 14370789) from the Ministry of Education, Culture, Sports, Science and Technology (MEXT), Japan, and by funds (No. 031001) from the Central Research Institute of Fukuoka University.

REFERENCES

Antonelli-Orlidge, A., Saunders, K. B., Smith, S. R., and D'Amore, P. A. (1989). An activated form of transforming growth factor β is produced by cocultures of endothelial cells and pericytes. *Proc. Natl. Acad. Sci. U.S.A.* **88:**4544–4548.

Bradford, M. M. (1976). A rapid and sensitive method for the quantitation of microgram quantities of protein utilizing the principle of protein-dye binding. *Anal. Biochem.* **72:**248–254.

Dehouck, M.-P., Jolliet-Riant, P., Brée, F., Fruchart, J.-C., Cecchelli, R., and Tillement, J.-P. (1992). Drug transfer across the blood–brain barrier: Correlation between in vitro and in vivo models. *J. Neurochem.* **58:**1790–1797.

Deli, M. A., Descamps, L., Dehouck, M.-P., Cecchelli, R., Joó, F., Ábrahám, C. S., and Torpier, G. (1995). Exposure of tumor necrosis factor-α to luminal membrane of bovine brain capillary endothelial cells cocultured with astrocytes induces a delayed increase of permeability and cytoplasmic stress fiber formation of actin. *J. Neurosci. Res.* **41:**717–726.

Dente, C. J., Steffes, C. P., Speyer, C., and Tyburski, J. G. (2001). Pericytes augment the capillary barrier in in vitro cocultures. *J. Surg. Res.* **97:**85–91.

Flanders, K. C., Ren, R. F., and Lippa, C. P. (1998). Transforming growth factor-βs in neurodegenerative disease. *Prog. Neurobiol.* **54:**71–85.

Fontaine, M., Elmquist, W. F., and Miller, D. W. (1996). Use of rhodamine 123 to examine the functional activity of P-glycoprotein in primary cultured brain microvessel endothelial cell monolayers. *Life Sci.* **59:**1521–1531.

Halstead, J., Kemp, K., and Ignotz, R. A. (1995). Evidence for involvement of phosphatidylcholine-phospholipase C and protein kinase C in transforming growth factor-β signaling. *J. Biol. Chem.* **270:**13600–13603.

Hartsough, M. T., and Mulder, K. M. (1995). Transforming growth factor β activation of $p44^{mapk}$ in proliferating cultures of epithelial cells. *J. Biol. Chem.* **270:**7117–24.

Orlidge, A., and D'Amore, P. A. (1987). Inhibition of capillary endothelial cell growth by pericytes and smooth muscle cells. *J. Cell Biol.* **105:**1455–1462.

Ramsauer, M., Krause, D., and Dermietzel, R. (2002). Angiogenesis of the blood-brain barrier in vitro and the function of cerebral pericytes. *FASEB J.* **16:**1274–1276.

Raub, T. J. (1996). Signal transduction and glial cell modulation of cultured brain microvessel endothelial cell tight junctions. *Am. J. Physiol.* **271:**C495–C503.

Rubin, L. L., and Staddon, J. M. (1999). The cell biology of the blood–brain barrier. *Annu. Rev. Neurosci.* **22:**11–28.

Sato, Y., and Rifkin, D. B. (1989). Inhibition of endothelial cell movement by pericytes and smooth muscle cells: activation of a latent transforming growth factor-β1-like molecular by plasmin during co-culture. *J. Cell Biol.* **109:**309–315.

Tatsuta, T., Naito, M., Mikami, K., and Tsuruo, T. (1994). Enhanced expression by the brain matrix of P-glycoprotein in brain capillary endothelial cells. *Cell Growth Differ.* **5:**1145–1152.

Tatsuta, T., Naito, M., Oh-hara, T., Sugawara, I., and Tsuruo, T. (1992). Functional involvement of P-glycoprotein in blood-brain barrier. *J. Biol. Chem.* **267:**20383–20391.

Utsunomiya, Y., Hasegawa, H., Yanagisawa, K., and Fujita, S. (1997). Enhancement of *mdrl* gene expression by transforming growth factor-β1 in the new adriamycin-resistant human leukemia cell line ME-F_2/ADM. *Leukemia* **11:**894–895.

Wang, W., Merrill, M. J., and Borchardt, R. T. (1996). Vascular endothelial growth factor affects permeability of brain microvessel endothelial cells in vitro. *Am. J. Physiol.* **271:**C1973–C1980.

Wrana, J. L., Attisano, L., Wieser, R., Ventura, F., and Massagué, J. (1994). Mechanism of activation of the TGF-β receptor. *Nature* **370:**341–347.

Cellular and Molecular Neurobiology, Vol. 24, No. 2, April 2004 (© 2004)

Uptake and Efflux of Quinacrine, a Candidate for the Treatment of Prion Diseases, at the Blood-Brain Barrier

Shinya Dohgu,[1,2] Atsushi Yamauchi,[2] Fuyuko Takata,[2] Yasufumi Sawada,[1] Shun Higuchi,[1] Mikihiko Naito,[3] Takashi Tsuruo,[3] Susumu Shirabe,[4] Masami Niwa,[4] Shigeru Katamine,[4] and Yasufumi Kataoka[2,5]

Received April 7, 2003; accepted May 22, 2003

SUMMARY

1. A clinical trial of quinacrine in patients with Creutzfeldt–Jakob disease is now in progress. The permeability of drugs through the blood–brain barrier (BBB) is a determinant of their therapeutic efficacy for prion diseases. The mechanism of quinacrine transport across the BBB was investigated using mouse brain endothelial cells (MBEC4).

2. The permeability of quinacrine through MBEC4 cells was lower than that of sodium fluorescein, a BBB-impermeable marker. The basolateral-to-apical transport of quinacrine was greater than its apical-to-basolateral transport. In the presence of P-glycoprotein (P-gp) inhibitor, cyclosporine or verapamil, the apical-to-basolateral transport of quinacrine increased. The uptake of quinacrine by MBEC4 cells was enhanced in the presence of cyclosporine or verapamil.

3. Quinacrine uptake was highly concentrative, this event being carried out by a saturable and carrier-mediated system with an apparent K_m of 52.1 μM. Quinacrine uptake was insensitive to Na^+-depletion and changes in the membrane potential and sensitive to changes in pH. This uptake was decreased by tetraethylammonium and cimetidine, a substrate and an inhibitor of organic cation transporters, respectively.

4. These findings suggest that quinacrine transport at the BBB is mediated by the efflux system (P-gp) and the influx system (organic cation transporter-like machinery).

KEY WORDS: quinacrine; blood–brain barrier; mouse brain endothelial cells; P-glycoprotein; organic cation transporter; Creutzfeldt–Jakob disease.

INTRODUCTION

Prion diseases including Creutzfeldt–Jakob disease (CJD) are progressive, fatal neurodegenerative diseases induced by conformational changes in prion protein (PrP) in

[1] Department of Medico-Pharmaceutical Sciences, Graduate School of Pharmaceutical Sciences, Kyushu University, Fukuoka, Japan.

[2] Department of Pharmaceutical Care and Health Sciences, Faculty of Pharmaceutical Sciences, Fukuoka University, Fukuoka, Japan.

[3] Institute of Molecular and Cellular Biosciences, University of Tokyo, Tokyo, Japan.

[4] Nagasaki University Graduate School of Biomedical Sciences, Nagasaki, Japan.

[5] To whom correspondence should be addressed at Department of Pharmaceutical Care and Health Sciences, Faculty of Pharmaceutical Sciences, Fukuoka University, 8-19-1 Nanakuma, Jonan-ku, Fukuoka 814-0180, Japan; e-mail: ykataoka@cis.fukuoka-u.ac.jp.

0272-4340/04/0400-0205/0

the central nervous system. It has been reported that quinacrine, an antimalarial drug, could rapidly eradicate production of the disease-associated and protease-resistant isoform of the prion protein (PrP^{SC}) in vitro (Korth *et al.*, 2001). A clinical trial of quinacrine has started at the Department of Neurology, Faculty of Medicine, Fukuoka University and the Department of Neurology, Faculty of Medicine, Nagasaki University. A transient improvement was observed in CJD patients (Follette, 2003).

The members of organic cation transporter (OCT) family include OCT1 (Grundemann *et al.*, 1994), OCT2 (Okuda *et al.*, 1996), OCT3 (Kekuda *et al.*, 1998), novel organic cation transporter (OCTN)1 (Tamai *et al.*, 1997), OCTN2 (Wu *et al.*, 1998), and OCTN3 (Tamai *et al.*, 2000). The tissue distribution patterns of the OCT family are dependent on the animal species. In the human and rat brain, OCT2 mRNA (Koepsell, 1998), OCTN1 mRNA (Tamai *et al.*, 1997; Wu *et al.*, 2000), and OCTN2 mRNA (Wu *et al.*, 1998, 1999) have been detected. OCTN1 and OCTN2 are expressed in the mouse brain (Tamai *et al.*, 2000). Immortalized rat brain endothelial cells (RBE4) express OCTN2 (Friedrich *et al.*, 2003). OCTN1 and OCTN2 are structurally much more closely related to each other than to OCT1, OCT2, and OCT3 (Wu *et al.*, 2000). Quinacrine is an organic cation and an organic base. The entry of organic cations such as choline into the brain occurs via transport systems present in the blood brain barrier (BBB) (Friedrich *et al.*, 2001; Sawada *et al.*, 1999). The transport of L-carnitine was mediated by OCTN2 in RBE4 cells (Friedrich *et al.*, 2003). Quinacrine inhibited tetraethylammonium (TEA) transport in MDCK cells expressing rat OCT2 (Sweet and Pritchard, 1999).

The BBB permeability of quinacrine is a determinant of its therapeutic efficacy for CJD. Quinacrine is known to pass through the BBB (Korth *et al.*, 2001), although the extent of quinacrine penetration into the brain and the mechanism involved in quinacrine transport across the BBB remain obscure. In this study, we investigated the properties of quinacrine transport into the brain using mouse brain capillary endothelial cells (MBEC4).

MATERIALS AND METHODS

Materials

Quinacrine dihydrochloride and sodium azide (NaN_3) were purchased from Tokyo Kasei Kogyo (Tokyo, Japan) and Kishida Kagaku (Osaka, Japan), respectively. N-Methylglucamine, 2,4-dinitrophenol (DNP), carbonyl cyanide *p*-(trifluoromethoxy) phenylhydrazone (FCCP), valinomycin, amiloride, tetraethylammonium (TEA), cimetidine, and verapamil were purchased from Sigma (St. Louis, MO). Cyclosporine was kindly supplied by Novartis (Basel, Switzerland). All other chemicals were commercial products of reagent grade.

Cell Culture

MBEC4 cells isolated from BALB/c mice brain cortices and immortalized by SV40-transformation (Tatsuta *et al.*, 1992) were cultured in Dulbecco's modified Eagle's medium (DMEM) (GIBCO BRL, Life Technologies, Grand Island, NY)

supplemented with 10% fetal bovine serum, 100 units/mL penicillin, and 100 μg/mL streptomycin in a humidified atmosphere of 5% CO_2/95% air at 37°C. For the transport experiments, MBEC4 cells (42,000 cells/cm^2) were plated into the collagen-coated polycarbonate membrane (1.0 cm^2, 3.0-μm pore size) of the Transwell™ insert (12-well type) (Costar, MA). For the cellular uptake experiments, cells were seeded at a density of 21,000 cells/cm^2 on 4- or 24-well multi dishes (Nunc, Roskilde, Denmark). MBEC4 cells were cultured for 3 days and then used for the following experiments. MBEC4 cells show both general brain endothelial and specific BBB characteristics including the expression of P-glycoprotein (P-gp) (Tatsuta *et al.*, 1992, 1994).

Transcellular Transport of Quinacrine Across MBEC4 Cells

To initiate the transport experiments, the medium was removed and cells were washed three times with Krebs-Ringer buffer (118 mM NaCl, 4.7 mM KCl, 1.3 mM $CaCl_2$, 1.2 mM $MgSO_4$, 1.0 mM NaH_2PO_4, 25 mM $NaHCO_3$, 11 mM D-glucose, pH 7.4). Krebs-Ringer buffer was applied on the outside of the insert in the well (abluminal side) (1.5 mL) and the luminal side of the insert (0.5 mL). Krebs-Ringer buffer containing 50–200 μM quinacrine (MW 473) or 100 μM sodium fluorescein (Na-F) (MW 376), a paracellular transport marker, was loaded on the luminal or abluminal side of the insert. Samples (0.5 mL) were removed from the luminal or abluminal chamber at 10, 20, 30, and 60 min and immediately replaced with fresh Krebs-Ringer buffer. The quinacrine concentration in the samples was determined using a multiwell fluorometer (Ex(λ) 450 nm; Em(λ) 530 nm) (CytoFluor Series 4000, PerSeptive Biosystems, Framingham, MA). Aliquots (5 μL) from the samples were mixed with 200 μL of Krebs-Ringer buffer and then the concentration of Na-F was measured (Ex(λ) 485 nm; Em(λ) 530 nm). Permeability coefficient and clearance were calculated according to the method described by Dehouck *et al.* (1992). Clearance was expressed as μL of tracer diffusing from the luminal to the abluminal chambers and was calculated from the initial concentration of tracer in the luminal chamber and the final concentration of tracer in the abluminal chamber: *Clearance* $(\mu L) = [C]_A \times V_A/[C]_L$ where $[C]_L$ is the initial luminal tracer concentration, $[C]_A$ is the abluminal tracer concentration, and V_A is the volume of the abluminal chamber. During the 60-min period of the experiment, the clearance volume increased linearly with time. The average volume cleared was plotted versus time, and the slope was estimated by linear regression analysis. The slope of clearance curves for the MBEC4 monolayer was denoted PS_{app}, where PS is the permeability × surface area product (in μL per min). The slope of the clearance curve with the control membrane was denoted $PS_{membrane}$. The real PS value for the MBEC4 monolayer (PS_{trans}) was calculated from $1/PS_{app} = 1/PS_{membrane} + 1/PS_{trans}$. The PS_{trans} values were divided by the surface area of the Transwell™ inserts to generate the permeability coefficient (P_{trans}, in cm per min).

Cellular Uptake of Quinacrine by MBEC4 Cells

For the uptake experiments, MBEC4 cells were washed three times with uptake buffer (143 mM NaCl, 4.7 mM KCl, 1.3 mM $CaCl_2$, 1.2 mM $MgSO_4$, 11 mM D-glucose,

10 mM HEPES, pH 7.4) and incubated with 0.5 mL of the uptake buffer containing quinacrine (1–200 μM) at 37°C for 1–120 min. After incubation, the buffer was removed and cells were washed three times with ice-cold phosphate-buffered saline. The cells were solubilized with 250 μL of 1 N NaOH. Aliquots of the cell solution were removed for protein assay according to the method of Bradford using a Bio-Rad protein assay kit (Bio-Rad Laboratories, Hercules, CA) (Bradford, 1976). Aliquots (200 μL) of the cell solution were neutralized with 200 μL of 1 N HCl and then sample fluorescence was measured (Ex(λ) 450 nm; Em(λ) 530 nm). Quinacrine uptake is expressed as the cell-to-medium ratio (quinacrine amounts in the cells/quinacrine concentration in the medium).

Estimation of Kinetic Parameters

The kinetic parameters for quinacrine uptake by MBEC4 cells were calculated by fitting the uptake rate (V) to the following equation: $V = (V_{max} \times S)/(K_m + S) + P_{dif} \times S$ where V_{max} is the maximum uptake rate of quinacrine (nmol/15 min/mg protein), S is the quinacrine concentration in the medium (μM), K_m is the Michaelis–Menten constant (μM), P_{dif} is the first-order constant for the nonsaturable component (μL/15 min/mg protein). Curve fitting was performed by the nonlinear least-squares regression program, MULTI (Yamaoka *et al.*, 1981).

Detection of OCTN1 mRNA

Total RNA from MBEC4 cells was extracted using TRIZOL™ reagent (Invitrogen, Carlsbad, CA). The primer pair used in the reverse transcription-polymerase chain reaction (RT-PCR) was designed based on the nucleotide sequence of the mouse OCTN1 transporter. The upper primer was 5′-CCTGTTCTGTGTTCCCC-TGT-3′ and the lower primer was 5′-GGTTATGGTGGCAATGTTCC-3′. The expected size of the RT-PCR product, predicted from the positions of the primers, was 232 bp. A SuperScript One-Step RT-PCR system (Invitrogen) was used for reverse transcription of RNA, and OCTN1 cDNA were amplified by PCR. Amplification was performed in a DNA thermal cycler (PC707; ASTEC, Fukuoka, Japan) according to the following protocol: cDNA synthesis for 30 min at 50°C, predenaturation for 2 min at 94°C; 40 cycles of denaturation for 30 s at 94°C, primer annealing for 30 s at 57°C, and polymerization for 30 s at 70°C; and final extension for 5 min at 72°C. Each 10 μL of PCR product was analyzed by electrophoresis on a 3% agarose (Sigma) gel with ethidium bromide staining. The gels were photographed under UV light using a DC290 Zoom digital camera (Kodak, Rochester, New York).

Statistical Analysis

The results are expressed as means ± SEM. Statistical analysis was performed using the Student's unpaired t test. The differences between means were considered to be significant when P values were less than 0.05.

RESULTS

The MBEC4 permeability coefficient of quinacrine dose-dependently increased from $0.58 \pm 0.025 \times 10^{-3}$ to $2.1 \pm 0.15 \times 10^{-3}$ cm/min, when the quinacrine concentration was increased from 50 to 200 μM. The MBEC4 permeability coefficient of quinacrine (100 μM) was significantly lower than that of Na-F (Fig. 1(A)). Permeability coefficients of the basolateral-to-apical transport of quinacrine and Na-F were $1.1 \pm 0.054 \times 10^{-3}$ and $1.5 \pm 0.17 \times 10^{-3}$ cm/min, respectively, while those of the apical-to-basolateral transport were $0.66 \pm 0.023 \times 10^{-3}$ and $1.5 \pm 0.25 \times 10^{-3}$ cm/min, respectively. The basolateral-to-apical transport of quinacrine was significantly higher than that in the opposite direction of transport (Fig. 1(B)). Cyclosporine (10 μM) and verapamil (20 μM) significantly increased the permeability coefficients of the apical-to-basolateral transport of quinacrine from $0.66 \pm 0.023 \times 10^{-3}$ to $1.15 \pm 0.056 \times 10^{-3}$ cm/min and from $0.57 \pm 0.034 \times 10^{-3}$ to $1.02 \pm 0.080 \times 10^{-3}$ cm/min, respectively (Fig. 1(C)).

Quinacrine uptake by MBEC4 cells was time-dependent and reached to the peak at 30 min after the exposure. The cell-to-medium ratio of quinacrine uptake was $2.37 \pm 0.18 \times 10^3$ μL/mg protein at 1 min after the exposure (Fig. 2(A)). Taking the finding that the cell volume of MBEC4 cells is approximately 3 μL/mg protein (Sawada *et al.*, 1999) into consideration, quinacrine is found to be extensively concentrated in MBEC4 cells. To determine whether this apparent concentrative uptake occurs due to only passive entry followed by intracellular binding, MBEC4 cells were treated with 0.015% Triton X for 10 min (Chan *et al.*, 1998). This treatment significantly reduced quinacrine uptake by 30–40% in the period between 30 and 60 min after the addition of quinacrine (Fig. 2(B)). These findings demonstrated that the apparent concentrative accumulation of quinacrine is not due only to passive entry followed by intracellular binding, because quinacrine, when actively accumulated in MBEC4 cells against a concentration gradient and unbound to the binding sites, leaks from cells into the external media through the permeabilized plasma membrane. The initial rate of quinacrine uptake by MBEC4 cells became saturated at 15-min after the exposure to quinacrine (1–200 μM) (Fig. 2(C)). Analysis of these data indicated the involvement of two transport processes (saturable carrier-mediated and nonsaturable system) in quinacrine uptake by MBEC4 cells. The parameters obtained by kinetic analysis were as follows; $V_{max} = 218 \pm 5.4$ nmol/15 min/mg protein, $K_m = 52.1 \pm 1.7$ μM, and passive permeability constant (P_{dif}) $= 94.3 \pm 1.7$ μL/15 min/mg protein.

Quinacrine uptake during a 15-min period was decreased by preincubation of the cells for 10 min with the metabolic inhibitors, NaN_3 (10 mM), DNP (1 mM), and FCCP (10 μM) (Table I). When the experiment was performed at 4°C, quinacrine uptake was reduced (Table I). This uptake was not affected by replacement of the external sodium with N-methylglucamine (Table I) or by changing the external potassium concentration (4.32 ± 0.09, 4.36 ± 0.19, and $4.62 \pm 0.25 \times 10^3$ μL/mg protein at 0, 4.7, and 100 mM of K^+, respectively) (Fig. 3(A)). Pretreatment of MBEC4 cells for a 10-min period with 10 μM of valinomycin, a K^+ ionophore, did not affect quinacrine uptake (Table I). This uptake was elevated from 1.54 ± 0.04 to $4.56 \pm 0.14 \times 10^3$ μL/mg protein by elevating the external pH from 6.4 to 8.4

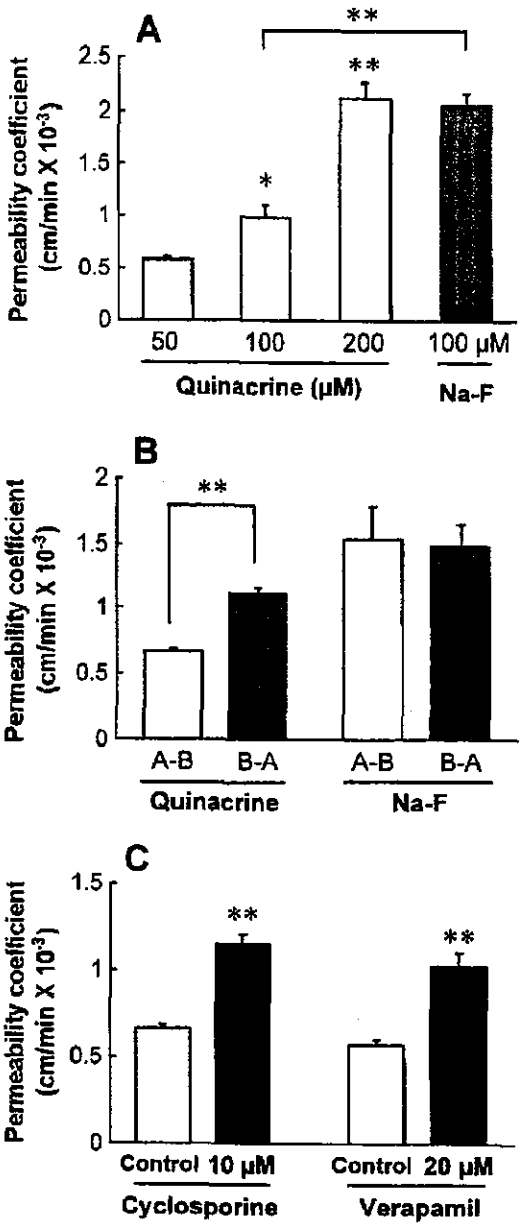

Fig. 1. Characteristics of quinacrine permeability through the MBEC4 monolayer. Panel (A), the permeability coefficients of quinacrine (50–200 μM) or Na-F (100 μM) through the MBEC4 monolayer. Panel (B), the permeability coefficients for the apical-to-basolateral ((A)–(B)) and basolateral-to-apical ((B)–(A)) transport of 100 μM quinacrine and 100 μM Na-F across the MBEC4 monolayer. (A)–(B) and (B)–(A) represent the blood-to-brain and brain-to-blood flux, respectively. Panel (C), the effects of 10 μM cyclosporine and 20 μM verapamil on the apical-to-basolateral transport of 100 μM quinacrine through the MBEC4 monolayer. The permeability coefficient of quinacrine was measured in the presence or absence of each drug. Values are means ± SEM. ($n = 3$–4 (A), 8 ((B), (C))). * $P < 0.05$ and ** $P < 0.01$; significant difference from the MBEC4 monolayer treated with 50μM quinacrine (A), the opposite direction (B), and the corresponding control (C).